SCIENTIFIC REPORTS

SUBJECT AREAS:
BIOPOLYMERS IN VIVO
ACTIN
NUCLEAR ENVELOPE
FOCAL ADHESION

Received
19 October 2012

Accepted
3 December 2012

Published
18 January 2013

Correspondence and requests for materials should be addressed to D.W. (wirtz@jhu.edu)

# The LINC-anchored actin cap connects the extracellular milieu to the nucleus for ultrafast mechanotransduction

Allison B. Chambliss[1,2], Shyam B. Khatau[1,2], Nicholas Erdenberger[1], D. Kyle Robinson[3], Didier Hodzic[4], Gregory D. Longmore[2,5] & Denis Wirtz[1,2]

[1]Department of Chemical and Biomolecular Engineering, The Johns Hopkins University, Baltimore, MD 21218, USA, [2]Physical Sciences - Oncology Center, The Johns Hopkins University, Baltimore, MD 21218, USA, [3]Department of Biomedical Engineering and Physical Sciences - Oncology Center, Oregon Health and Science University, Portland, OR 97006, USA, [4]Department of Ophthalmology, Washington University School of Medicine, St. Louis, MO 63110, USA, [5]Departments of Medicine and Cell Biology and Physiology and BRIGHT Institute, Washington University School of Medicine, St. Louis, MO 63110, USA.

**Cells continuously sense and respond to external mechanical forces through their cytoskeleton. Here we show that only a small subset of actin fibers, those forming the perinuclear actin cap that wraps around the nucleus, form in response to low physiological mechanical stresses in adherent fibroblasts. While conventional basal stress fibers form only past a threshold shear stress of 0.5 dyn/cm$^2$, actin-cap fibers are formed at shear stresses 50 times lower and orders-of-magnitude faster than biochemical stimulation. This fast differential response is uniquely mediated by focal adhesion protein zyxin at low shear stress and actomyosin fibers of the actin cap. We identify additional roles for lamin A/C of the nuclear lamina and linkers of nucleus to cytoskeleton (LINC) molecules nesprin2giant and nesprin3, which anchor actin cap fibers to the nucleus. These results suggest an interconnected physical pathway for mechanotransduction, from the extracellular milieu to the nucleus.**

A wide range of cells, including endothelial cells[1,2], lymphocytes[3,4], stem cells[5,6], chondrocytes[7], and fibroblasts[8] have the ability to sense and respond to external flow forces. Mechanical stresses induced by flow play a critical role in a multitude of important cell functions, both in normal and disease states. For instance, hemodynamic flow, which corresponds to shear stresses between 1 to 6 dyn/cm$^2$ (0.1–0.6 Pa) for veins and 10 to 70 dyn/cm$^2$ (1–7 Pa) for arteries[9], induces changes in endothelial gene expression and leukocyte attachment and rolling onto blood vessel walls[10], mediates the transport of immune and circulating tumor cells during inflammatory responses and cancer metastasis, and induces the activation of chondrocytes in the bone[7]. Interstitial flow through connective tissues, which corresponds to much lower shear stresses of $<$1 dyn/cm$^2$ [11], couples to chemoattractant gradients that enhance cancer metastasis[12,13]. How low and high stress stresses are transduced from the extracellular milieu all the way to the genome remains unclear.

Different mechano-active structures mediating two non-mutually exclusive modes of mechanotransduction from the extracellular milieu to the cytoplasm have been identified: ion channels, which stretch under shear forces, and focal adhesions[14,15], discrete protein clusters located at the basal surface of adherent cells, which grow in size and change the phosphorylation of their components under external shear. Focal adhesions tether the basal cell surface to the extracellular matrix through integrins which dynamically bind actin filaments by linker proteins including talin, vinculin, and zyxin[16]. Focal adhesions terminate contractile stress fibers that lie at the basal cellular surface. However, basal stress fibers do not connect directly to the nucleus[17,18], which eliminates the possibility that basal stress fibers could be part of a contiguous physical pathway that would connect focal adhesions to the nuclear genome.

In addition to basal stress fibers, highly organized, dynamic, oriented, thick actin cables tightly cover the apical surface of the interphase nucleus in adherent cells, forming the perinuclear actin cap[17,19,20]. While conventional stress fibers are confined to regions in the lamella and are few underneath the nucleus, the perinuclear actin cap is composed of actin filament bundles that cover the top of the interphase nucleus[17]. Actin cap fibers are terminated by their own focal adhesions, which are distinct from conventional focal adhesions and have been shown to dominate mechanosensing of substrate compliance[20]. Moreover, unlike conventional cortical actin, such as dorsal and basal stress fibers[21], the stress fibers of the actin cap are tightly connected to the apical surface of the

nucleus[17,19,22] through linkers of nucleus and cytoskeleton (LINC) complexes, which include nesprins, lamins, and SUN proteins[23–25]. LINC complexes mediate interconnections between the nucleus and the cytoskeleton. LINC proteins nesprin2giant, SUN2, and Samp1 have been shown to colocalize with actin near the nucleus and modulate nuclear movement in polarizing fibroblasts[24,26], while nesprin3 is necessary for actin remodeling and cell polarization in response to shear stress[27]. Importantly for this study, the LINC complex has been implicated in force transmission among the nucleus and the cytoskeleton[28]. The absence of LINC complexes in laminopathic models results in the disappearance of actin caps, without significantly affecting conventional stress fibers[21]. We hypothesized that the fibers that make up the perinuclear actin cap would be a critical component of a contiguous physical pathway connecting focal adhesions to the nuclear genome.

Here we show that cellular mechanotransduction by adherent cells in response to low shear stresses is largely dominated by the small and distinct subset of actin filaments that form the perinuclear actin cap. Actin-caps are formed by flow-induced shear stress. These results suggest an interconnected physical pathway for cellular mechanotransduction, from the extracellular milieu to the nucleus via focal adhesion proteins zyxin (but not FAK) at low shear stress and talin at high shear stress, actomyosin fibers of the actin cap, LINC complex-associated molecules nesprin2giant and nesprin3 to the nuclear envelope, and lamin A/C.

## Results

**Formation of the perinuclear actin cap induced by shear flow.** To assess whether mechanical stimulation would affect basal fibers and actin-cap fibers differently and to begin with a cellular state with little or no organized actin filament structure, mouse embryonic fibroblasts (MEFs) or C2C12 mouse mybolasts were serum-starved for two days before being subjected to shear-flow stimuli of controlled duration and flow rate (and therefore wall shear stress). Before application of shear flow, confocal microscopy was used to visualize cellular actin organization across the height of the cells, which were stained with phalloidin (Fig. 1, A-C). For most cells, there was actin on the apical surface of the interphase nucleus; however, actin filaments appeared disorganized, and any hint of aligned fibers was largely absent (Fig. 1C). Similarly, basal stress fibers were absent (Fig. 1A). Quantitative fluorescence microscopy showed that the vast majority of cells showed either no actin cap or a disorganized actin cap at the apical surface of the nucleus and also displayed little or no stress fibers at the basal surface of cells (Fig. 1, D-I). This constitutes the initial cellular state of all our subsequent studies.

The percentage of cells showing an organized actin cap increased by 50% within just 30 s of application of an exceedingly low shear stress of only 0.05 dyn/cm$^2$ (on the order of the shear stress induced by physiological interstitial flow) compared to unsheared cells placed in the same chamber (Fig. 2, A–D; solid curve in Fig. 2L). This shear stress approximately corresponds to a force of 50 pN applied to the cell's apical surface of 100 μm$^2$. During the same duration of applied flow, the percentage of cells showing organized conventional stress fibers at the basal surface remained unchanged and low ($<$ 20%; Fig. 2, G–I; solid curve in Fig. 2M), similar to the percentage of unsheared cells showing organized basal stress fibers placed in the same chamber for the same duration. The increased percentage of sheared cells subjected to the low shear stress of 0.05 dyn/cm$^2$ that showed an organized actin cap reached a steady state only after 5 min (solid curve Fig. 2L). The associated halftime for the formation of actin caps in sheared cells was just 2 min (solid curve in Fig. 2L). In comparison, during the same duration and magnitude of applied shear stress, the percentage of cells displaying organized basal stress fibers was unchanged compared to the no-shear case and remained low and unchanged for times as long as 30 min of shear flow (solid curve in Fig. 2M). We note that no preferential orientation or realignment of fibers, at neither the actin cap nor basal actin levels, was observed for up to our highest shear stress (5 dyn/cm$^2$) and longest shear time (30 min).

Together these results reveal that: (1) Only a small subset of actin fibers become organized in response to low shear stresses, those exclusively formed on top of the nucleus, while no new actin fibers are formed at the basal or dorsal cellular surfaces. (2) The formation of organized actin caps is extremely fast, taking place after $<$ 1 min of shear stimulation, and a steady state number of cells showing organized actin caps is reached within 5 min with a halftime of 2 min, while no significant increase in percentage of cells showing organized basal stress fibers is observed.

We additionally quantified actin cap and basal actin organization in non-serum-starved cells in 10% serum conditions (see Supplementary Fig. S1 online) before and after shear. We observed slight increases in actin cap and basal actin organizations after shear at 5 dyn/cm$^2$. However, these data were hardly significant, as the cells displayed high levels of actin organization without serum-starvation and before shear and therefore had little room to organize further.

**Actin cap fibers are selectively formed even at the lowest measureable shear stress, while basal stress fibers are formed only past a higher threshold shear stress.** We asked whether the formation of actin caps and basal stress fibers in cells subjected to shear flow depended on the level of shear stress. The serum-starved cells were subjected to shear stress for 0 to 30 min over three orders of magnitude of shear stress, ranging between 0.01 dyn/cm$^2$ and 10 dyn/cm$^2$, representing the physio-pathological range of shear stresses in interstitial flow in connective tissues (0.01–0.05 dyn/cm$^2$) and hemodynamic flow in veins and arteries (1–10 dyn/cm$^2$). The percentage of cells showing an organized perinuclear actin cap and/or organized basal stress fibers was measured as a function of the duration of shear (Fig. 2N). Surprisingly, significant actin cap formation occurred at all tested shear stresses (green curve in Fig. 2N). Indeed, no minimum (measurable) threshold shear stress seemed to be required to trigger the formation of actin caps in sheared cells, as a shear stress as low as 0.01 dyn/cm$^2$ was sufficient to induce a significant increase in the number of cells with an actin cap, within less than 5 min, compared to control unsheared cells kept in the same chamber for the same time. Moreover, no maximum shear stress induced destruction or damage in actin caps, at least up to shear stresses for which cells started to detach from their substratum (here, 10 dyn/cm$^2$). Hence, shear-induced actin cap formation was largely independent of the magnitude of applied shear stress.

In striking contrast to actin cap formation, we did not observe the formation of basal stress fibers at low shear stresses even for long durations of shear (purple curve in Fig. 2N). Rather, basal stress fiber formation was only triggered past a threshold value of shear stress of about 1 dyn/cm$^2$, i.e. a shear stress at least 100 fold higher than that required for inducing the formation of actin caps. Beyond this threshold shear stress, the percentage of cells showing organized basal stress fibers did not significantly further increase (Fig. 2N); moreover, the percentage of cells with organized basal stress fibers was largely independent of the duration of shear (dashed curve in Fig. 2M). We note that a relatively large percentage of cells showed an organized actin cap while showing no organized basal stress fibers, as high as 23% (~65% of cells with organized caps) for a shear stress of 0.05 dyn/cm$^2$ (Fig. 2O).

The curves measuring the percentage of cells with an actin cap as a function of shear duration at different shear stresses did not collapse into a single master curve when plotted as a function of the product of shear stress and duration of shear (not shown), which suggests that actin cap formation depends on both the duration and the magnitude of shear stress independently. Indeed, while shear duration modulated actin cap formation, shear stress levels did not. Together these

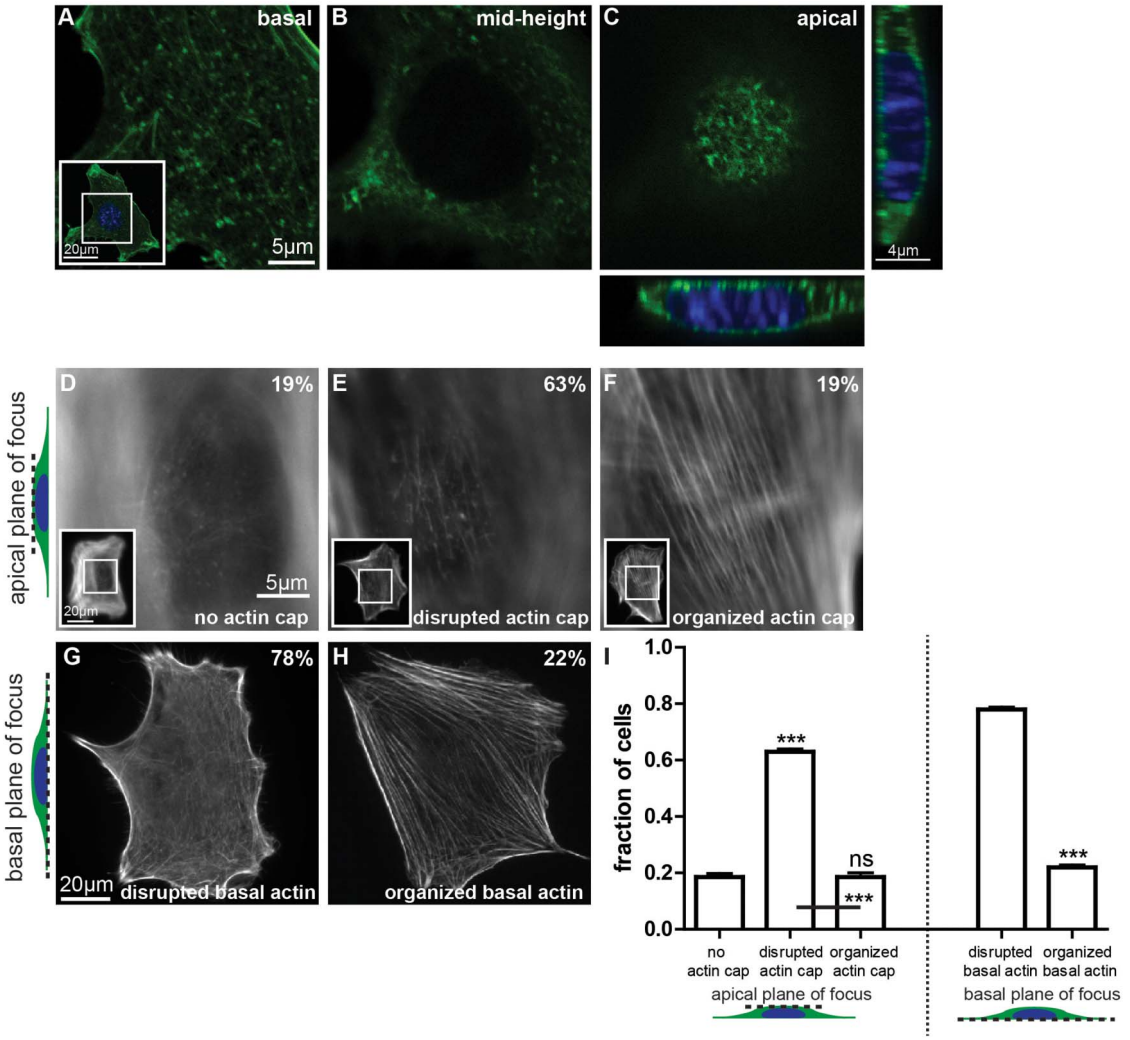


**Figure 1 | Defining the architecture of the perinuclear actin cap.** (A–C). Confocal fluorescent micrographs of the actin filament network obtained at the basal surface, mid-height, and the apical surface of wildtype MEFs in serum-starved conditions. Inset shows the whole imaged cell at the basal surface, with the inner white box framing the zoomed region shown in the main panels. Thin confocal cross-sections along (far right panel) and perpendicular to (bottom panel) the actin cap direction show a bulging nucleus. Cross-sections were expanded 1.5 fold in the apical direction of the cell to aid visualization. (D–F). Conventional epifluorescence microscopy focusing on the top of the nucleus can readily reveal either the total absence of an organized perinuclear actin cap (D), a disrupted actin cap (E), or a highly organized perinuclear actin cap (F). Insets show the whole imaged cell at the apical surface, with inner white boxes framing the zoomed regions shown in the main panels. (G) and (H). Architecture of basal actin stress fibers, which are either disrupted/rare (G) or organized (H). Numbers shown in the top right corner of the panels correspond to the percentage of cells showing that particular actin organization (see panel I). For all images in this figure, F-actin is visualized with phalloidin. (I). Percentages of cells displaying an organized perinuclear actin cap, a disrupted actin cap, or no actin cap (left graph) or organized or disrupted basal actin (right graph). Significance stars indicate differences between bars and the first bar in the set, unless otherwise noted, using a one-way ANOVA test or a t-test. On the graphs, *** and ns indicate p value $<0.001$ and $>0.05$, respectively. $\alpha=0.05$ was used for all significance tests. Three independent experiments were conducted to quantify a total of 150 cells.

results suggest that actin cap fibers and basal stress fibers are formed in qualitatively different ways: actin caps are formed rapidly at all measurable levels of shear stress, while conventional basal stress fibers are formed only past a high shear-stress threshold.

**Shear stimulation is significantly more potent than serum stimulation and actin cap relaxation.** To place this rapid and distinct formation of actin caps by mild mechanical stimulation in perspective, we also assessed actin cap formation following biochemical stimulation of cells by adding serum to the medium of unsheared serum-starved cells. In the absence of flow, serum addition did not trigger the formation of additional basal or apical actin filament bundles for times up to the same time used for shear experiments, 1–30 min (Fig. 3A). Hence the rate of shear-stress-induced formation of actin caps in adherent cells (~30 s, Fig. 2L) is orders-of-magnitude faster than the rate of formation of actin caps following biochemical stimulation (> 48 h; Fig. 3A).

Next, we assessed the stability of actin cap structures formed during mechanical stimulation once shear stress was ended. We also compared the rates of disassembly of actin caps following biochemical de-stimulation (serum-starvation) and following physical de-stimulation (cessation of shear flow). We found that actin caps that had been formed during shear for 30 min disappeared exponentially within 1 h, i.e. more slowly than it took them to be formed by an applied shear flow, yet more rapidly than for basal stress fibers to disappear (Fig. 3C). The rate of decrease in the percentage of cells with an organized actin cap was about 3.6 $h^{-1}$, while this rate was 1.2 $h^{-1}$ for a similar decrease in the percentage of cells with organized basal stress fibers (Fig. 3D). Moreover, the rate of actin cap disassembly upon flow cessation was significantly faster than the rate of actin

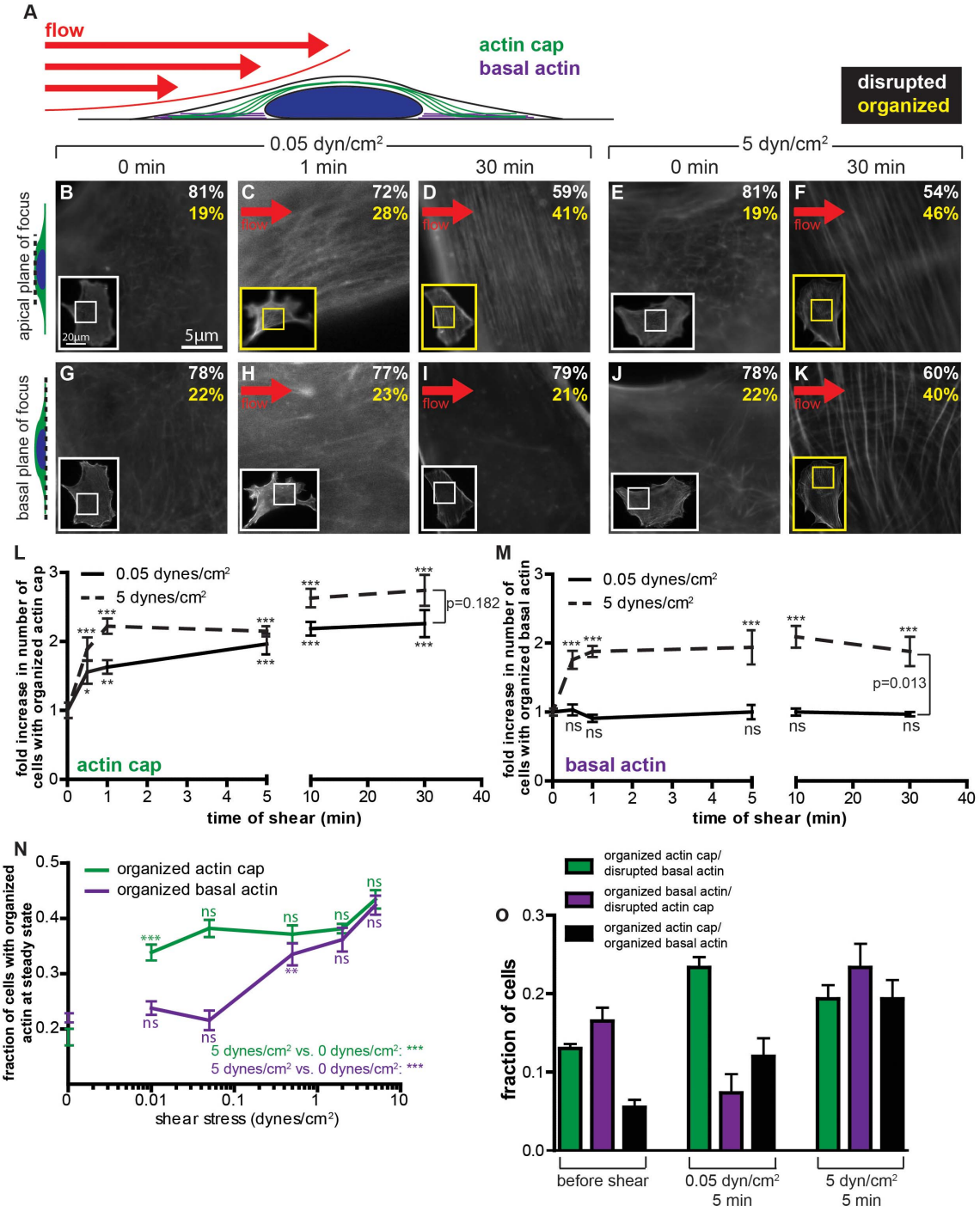


**Figure 2 | Formation of the actin cap is induced more rapidly and at lower shear stresses than formation of basal actin.** (A). Schematic of an adherent cell subjected to flow of controlled shear stress for a controlled duration. Status of actin organization at the apical (green) and basal (purple) surface is examined by fluorescence microscopy. (B–K). Typical actin organization on top of the nucleus (B–F) and at the basal surface (G–K) before shear (0 min), after 1 or 30 min of low shear stress (0.05 dyn/cm$^2$), and after 30 min of higher shear stress (5 dyn/cm$^2$). White and yellow text corresponds to the percentage of cells with disrupted and organized actin, respectively, after shear. Insets show the whole cell, with inner boxes framing the zoomed regions shown in the main panels. (L) and (M). Fold increase in the number of cells showing organized actin caps (L) or basal actin (M) as a function of time for shear stresses of 0.05 dyn/cm$^2$ (solid) and 5 dyn/cm$^2$ (dashed), as compared to cells in no-shear conditions (0 min). Stars indicate statistically significant differences in the percentages of cells between the time of shear considered and the condition at time 0 using two-way ANOVA tests. (N). Percentage of cells with organized actin caps (green) or basal actin (purple) as a function of shear stress for a duration of shear that corresponded to a steady state of actin cap or basal actin organization. Stars indicate statistically significant differences for the level of shear stress considered and the previous lower value of shear stress, unless otherwise indicated, using a one-way ANOVA test. (O). Percentages of cells showing various combinations of basal actin and actin cap organization before shear (far left) and either after low shear stress (middle) or higher shear stress applications (far right). The remaining percentages exhibited both disrupted basal actin and disrupted apical actin caps. For all data shown, ***, **,*, and ns indicate p value $<0.001$, $<0.01$, $<0.05$, and $>0.05$, respectively. $\alpha=0.05$ was used for all significance tests. Three independent experiments were conducted to quantify a total of 150 cells per condition.

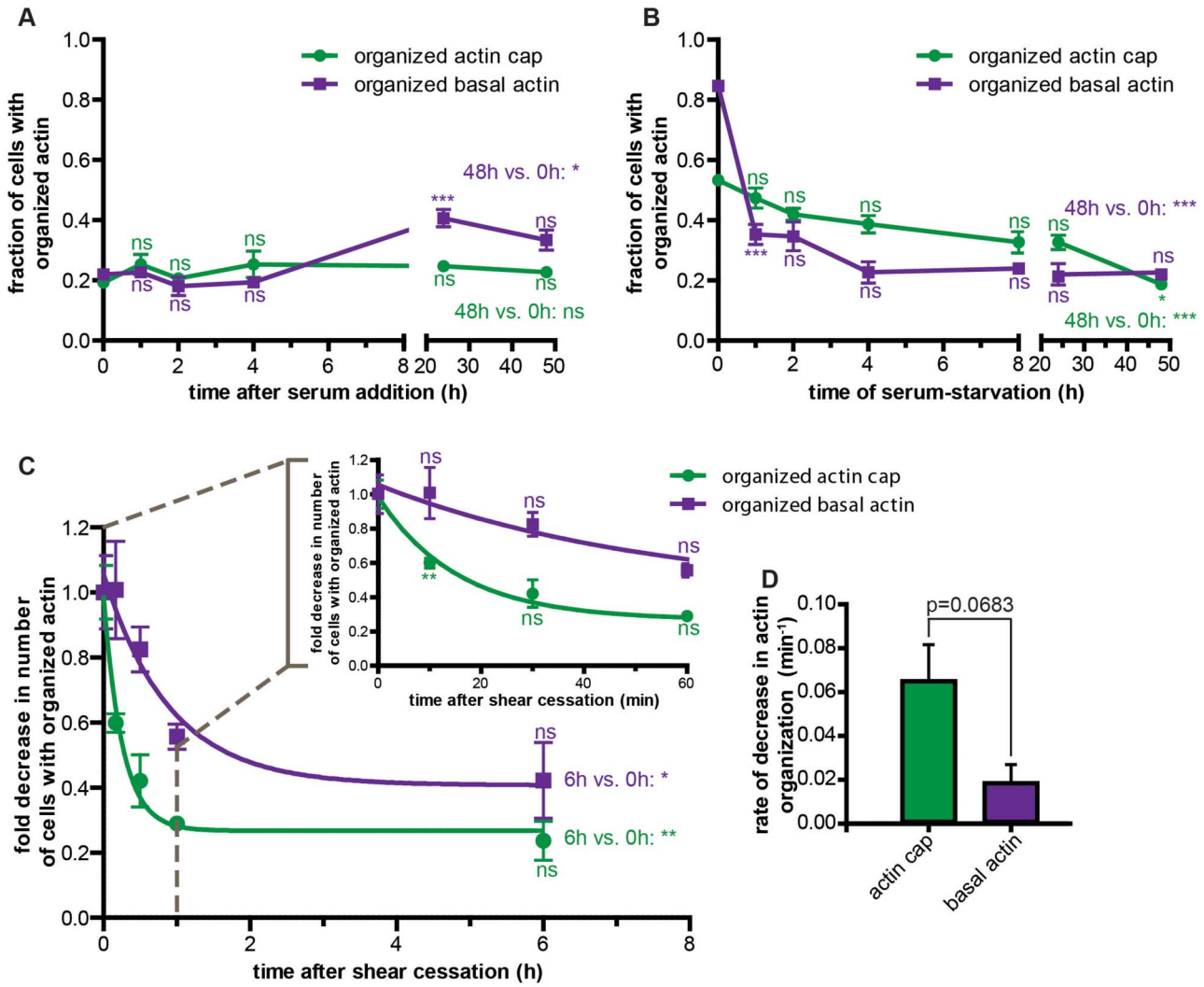


**Figure 3 | Actin cap dynamics following mechanical stimulation are significantly faster than following biochemical stimulation.** (A) and (B). Percentages of cells showing an organized actin cap (green curves) and organized basal stress fibers (purple curves) after either switching to serum-starved conditions following regular cell culture with serum (B), or serum addition following 2-day serum-starvation (A). (C). Fold decrease in the number of cells with organized actin caps (green curve) and organized basal stress fibers (purple curve) following the cessation of shear. Inset shows early kinetics. (D). Rates of decay in the percentages of cells with organized actin caps (green bar) and organized basal stress fibers (purple bar) upon cessation of shear. For all curves in this figure, significance stars just above or below data points compare the considered time point to the time point just before it using one-way ANOVA tests. Significances on far right of graphs indicate differences between the last time points and the first time points, as indicated. ***, **,*, and ns indicate p value $<0.001$, $<0.01$, $<0.05$, and $>0.05$, respectively. $\alpha=0.05$ was used for all significance tests. Three independent experiments were conducted to quantify a total of 150 cells per condition.

cap disassembly following the sudden switch from in-serum conditions to serum-starved conditions (Fig. 3B), 40 min *vs.* > 20 h.

These results indicate that the application and cessation of shear stress are significantly more potent types of cellular stimulation and de-stimulation than biochemical activation/de-activation by addition/removal of serum to induce actin filament re-organization, in particular on the apical surface of the nucleus. Moreover, actin caps are significantly more unstable than basal stress fibers upon flow cessation with a much shorter turnover time than basal stress fibers.

**Shear-induced actin cap formation is mediated by zyxin at low shear and talin at high shear.** Like basal actin fibers, nuclear actin cap fibers are terminated by associated focal adhesions[20]. Therefore, we hypothesized that components of focal adhesions would mediate actin cap formation induced by flow shear stress. To test this hypothesis, cells were depleted of major focal adhesion protein talin, as well as focal adhesion proteins believed to play a role in mechanotransduction including zyxin and FAK[29–34], using shRNA technology. In the absence of shear, the depletion of talin, zyxin, and FAK had little to no significant effect on the few actin cap and basal stress fibers in those cells compared to control cells transfected with firefly luciferase shRNA (Fig. 4, A–C, black bars, inset panels). In contrast, under both low and high shear stress stimulation, cells depleted of talin showed no significant actin cap formation in distinct contrast to control sheared cells (Fig. 4B, main panel). Depletion of FAK did not affect shear-induced actin cap formation. Interestingly, zyxin depletion blocked actin cap formation only in cells subjected to low shear stress, not high shear stress. This shear-stress dependent role of zyxin was further verified with cells transfected with another shRNAi zyxin construct and subjected to the same functional analysis.

Since focal adhesion formation involves actomyosin contractility[34], we asked whether actomyosin contractility was required for actin cap formation induced by shear. We found that treatment of cells with myosin light chain kinase (MLCK) inhibitor ML7, myosin

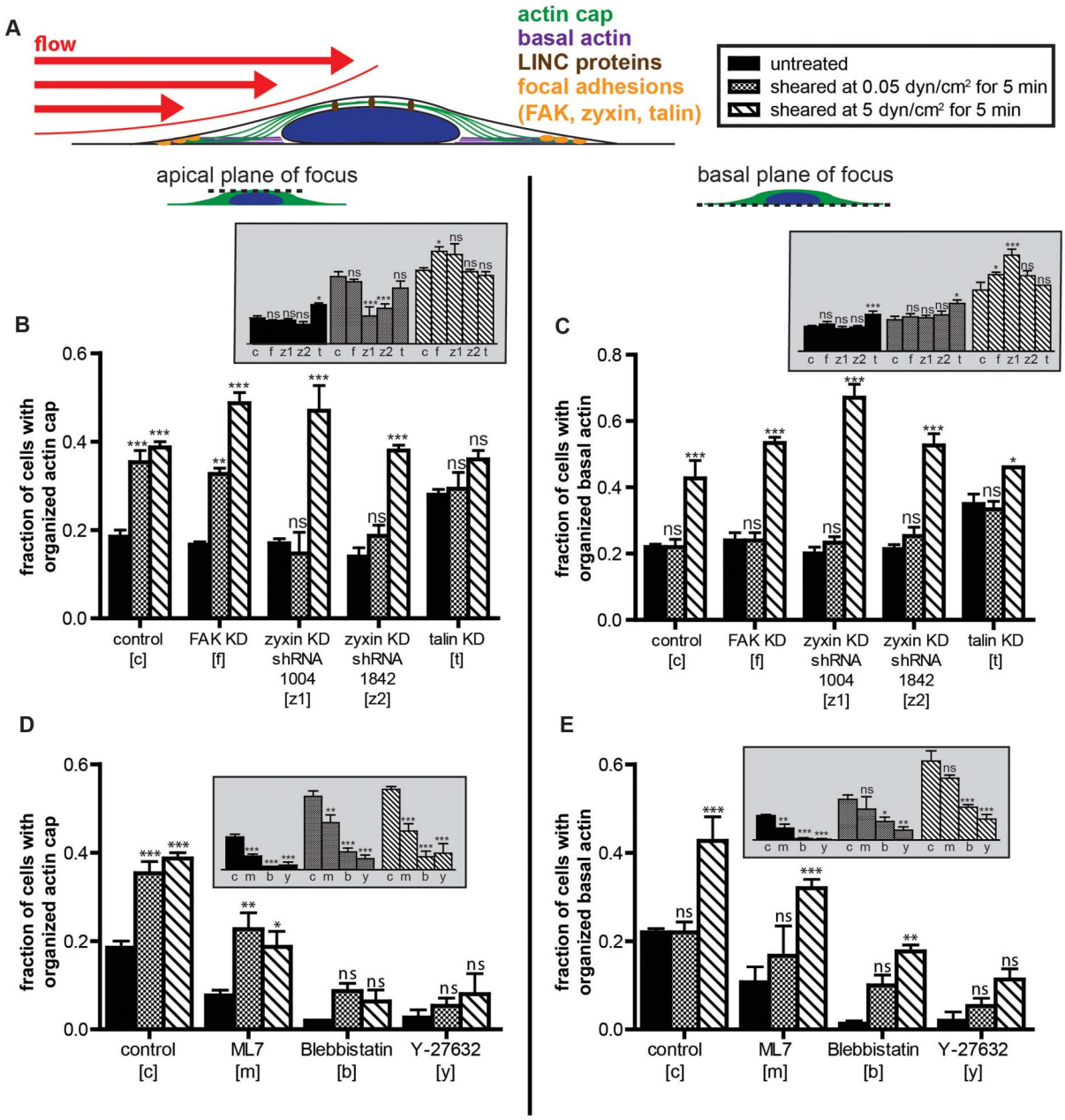


**Figure 4 | Shear-induced actin cap formation is mediated by zyxin at low shear stress and talin at high shear stress.** (A). Schematic of an adherent cell subjected to a shear flow of controlled flow rate applied for a controlled duration. Focal adhesion proteins (shown in orange) and LINC complex proteins (shown in brown, see Fig. 5) were knocked down or knocked out and the resulting cells were exposed to shear flow. Status of the actin filament network at the apical surface of the nucleus and the basal surface of the cells is examined by epifluorescence microscopy. (B) and (C). Percentages of control and focal adhesion knockdown MEFs featuring an organized actin cap (B) and organized basal stress fibers (C) in cells with the absence/presence of shear flow of shear stresses of 0.05 dyn/cm$^2$ and 5 dyn/cm$^2$ applied for 5 min. Cells were separately shRNA-depleted of focal adhesion proteins FAK, zyxin, or talin. (D) and (E). Percentages of control and actomyosin contractility drug-treated MEFs featuring an organized actin cap (D) and organized basal stress fibers (E) in cells with the absence/presence of shear flow of shear stresses of 0.05 dyn/cm$^2$ and 5 dyn/cm$^2$ applied for 5 min. Cells were treated with the drugs ML-7 to inhibit myosin light chain kinase, blebbistatin to inhibit myosin II, and Y-27632 to inhibit Rho-kinase. For all main panel graphs, significances compare unsheared cells (black bars) to sheared cells (patterned bars) using two-way ANOVA tests. Inset graphs show the same bars but compare differences among different knockdown strains/drug treatments subjected to the same shear stress. For all data shown, ***, **,*, and ns indicate p value $<0.001$, $<0.01$, $<0.05$, and $>0.05$, respectively. $\alpha=0.05$ was used for all significance tests. Three independent experiments were conducted to quantify a total of 150 cells per condition.

II inhibitor blebbistatin, and Rho-kinase (ROCK) inhibitor Y-27632 all greatly reduced the percentage of cells showing an actin cap and basal stress fibers (Fig. 4, D and E, black bars, inset panels). Upon shear stimulation, myosin II, MLCK, and ROCK inhibition largely prevented the formation of actin caps (Fig. 4D, main panel) and, to a lesser extent, the formation of actin filament bundles at the basal cellular surface (Fig. 4E). For instance, myosin II inhibition with blebbistatin abrogated actin-cap response at both low and high shear stresses, but still allowed for basal stress fiber formation at high shear stress (Fig. 4, D and E).

**Shear-induced actin cap formation is mediated by LINC complexes that connect the actin cap to the nuclear lamina.** Our results would predict that actin cap formation would be abrogated in cells having a limited ability to form actin caps, such as lamin A/C-deficient (*Lmna*$^{-/-}$) cells[17]. In the absence of flow, < 3% of lamin A/C-deficient cells showed an organized perinuclear actin cap. As predicted, we found that actin caps in lamin A/C-deficient cells were not induced when these cells were subjected to shear flow corresponding to both low and high shear stress levels (Fig. 5, A and B).

Actin caps are absent from lamin A/C-deficient cells because actin-binding LINC complex molecules nesprin2giant and nesprin3, which specifically connect the actin cap to the nuclear lamina, cannot properly localize at the nuclear envelope[35,36] (Fig. 4A). We tested the hypothesis that LINC complexes mediated shear-induced actin cap formation by examining cells stably depleted of either nesprin2giant or nesprin3 (Fig. 5, C and D), which binds actin filaments to the nuclear lamina via SUN proteins[25]. Unlike control cells, nesprin-depleted cells showed no significant formation of actin caps upon shear stimulation (Fig. 5C), with a larger defect in nesprin3-depleted versus nesprin2giant-depleted cells. These results suggest that both LINC complexes and an intact nuclear lamina are required for the anchorage/formation of actin-cap fibers to the apical surface of the nucleus and subsequent stabilization by shear flow stimulation, and highlight the distinctive response of actin-cap fibers compared to conventional stress fibers.

## Discussion

Mechanical forces play a critical role in a wide range of normal functions of the cell, including cell differentiation, cell motility and homeostasis, as well as in disease conditions, including muscular dystrophy and cancer growth and metastasis. How extracellular forces are transduced from the extracellular milieu to the nuclear genome remains poorly understood. In particular, whether a physical

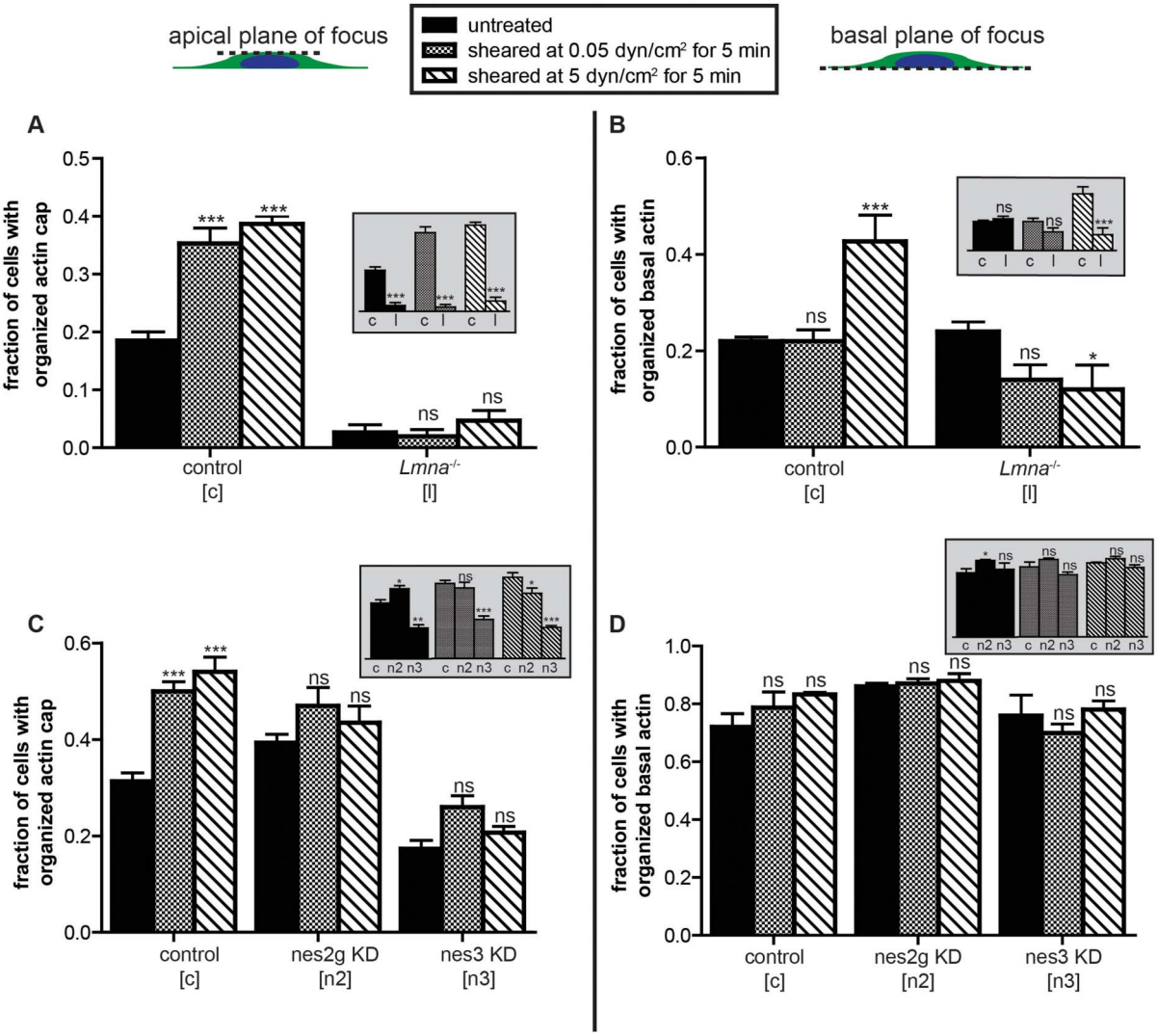


**Figure 5 | Shear-induced actin cap formation is mediated by LINC complexes and nuclear lamin A/C.** (A) and (B). Percentages of *Lmna*$^{+/+}$ and *Lmna*$^{-/-}$ MEFs featuring an organized actin cap (A) and organized basal stress fibers (B) in cells cultured in the absence/presence of shear flow of shear stresses of 0.05 dyn/cm$^2$ and 5 dyn/cm$^2$ applied for 5 min. Significances in main panels compare unsheared cells (black bars) to sheared cells (patterned bars). Inset graphs show same bars but compare differences between *Lmna*$^{+/+}$ and *Lmna*$^{-/-}$ cells within the same shear condition.
(C) and (D). Percentages of scramble control, nesprin2giant, and nesprin3 knockdown C2C12 cells featuring an organized actin cap (C) and organized basal stress fibers (D) in cells with the absence/presence of shear. Significances in main panels compare unsheared cells (black bars) to sheared cells (patterned bars) using two-way ANOVA tests. Inset graphs show same bars but compare differences between control and nesprin knockdown cells subjected to the same shear stress. For all data shown, ***, **,*, and ns indicate p value <0.001, <0.01, <0.05, and >0.05, respectively. $\alpha$=0.05 was used for all significance tests. Three independent experiments were conducted to quantify a total of 150 cells per condition.

pathway – as opposed to a biochemical pathway – that could contiguously transduce mechanical forces from the extracellular milieu to the nucleus exists is unclear. Due to its connectivity, such a physical pathway could mediate quick cellular responses to extracellular forces.

Here our results suggest that a small subset of actin fibers, those uniquely connected to the nuclear envelope through LINC complex molecules nesprin2giant and nesprin3 and forming the perinuclear actin cap, dominate cytoskeletal responses to low physiological stresses. At shear stresses as low as 0.01 dyn/cm$^2$, comparable to low shear stresses induced by interstitial flow in connective tissues, actin cap fibers form within 30 s, which was found to be orders-of-magnitude faster than biochemical stimulation with serum addition. Moreover, fibers of the perinuclear actin cap can disassemble upon flow cessation many orders-of-magnitude faster than following serum starvation.

Our results indicate that actin cap fibers respond more rapidly and more dynamically to shear flow than conventional actin stress fibers at the basal surface of cells. These basal fibers only assemble for flow-induced shear stresses at least 50 times larger than required for the formation of actin cap fibers, comparable to shear stresses induced by blood flows. This biphasic response is mediated by focal adhesion protein zyxin at low shear stresses, but not at high shear stresses. Additionally, we observed an ~80% recovery in organized actin caps – from ~50% before serum-starvation (Fig. 3B) to ~20% after serum-starvation (Fig. 3B) to ~40% after application of maximum shear (Fig. 2N). At the basal actin level, we only observed a ~50% recovery in stress fibers – from ~80% before serum-starvation (Fig. 3B) to ~20% after serum-starvation (Fig. 3B) to ~40% after application of maximum shear (Fig. 2N).

Our results suggest the possible existence of an entirely physical pathway for the transduction of mechanical forces from the extracellular milieu to the nuclear genome. This physical pathway contains five contiguous subcellular elements: actin-cap associated focal adhesions terminating contractile perinuclear actin cap fibers[20], which are anchored to the nuclear envelope through nesprin2giant and nesprin3 of LINC complexes at the nuclear envelope, which are in turn connected to the nuclear lamina and genome through SUN proteins via KASH-SUN protein interactions and lamin A/C.

We have recently shown that focal adhesions connected specifically to the actin cap (actin cap associated focal adhesions, or ACAFAs) are involved in cell mechanosensing over a wide range of substrate stiffnesses[20]. Interestingly, depletion of zyxin had no significant effect on the response of ACAFAs to changes in substrate compliance compared to control cells, while FAK was found to be a key mediator for mechanosensing. In our current work, actin cap formation was regulated by zyxin at low shear, while FAK did not play a role at any tested shear stress. Therefore, we speculate that FAK has a larger mechanosensing role, while zyxin has a larger mechanotransducing role. This role for zyxin is consistent with previous works including Yoshigi et al.[30] Our results concerning focal adhesion protein talin also raise interesting questions. Cells depleted of talin showed no significant actin cap formation in response to shear. However, talin-depleted cells also surprisingly showed a slightly higher percentage of cells with organized actin caps compared to control cells. In this respect, talin could also be considered an inhibitor of actin cap formation. Because the knockdown increased the number of actin caps before shear, it is possible that shearing was not sufficient to increase actin cap formation any further.

We also note that we observed a lower impact of nesprin2giant depletion than nesprin3 depletion when quantifying actin organization in response to shear flow. This is interesting, as nesprin2giant is known to have an actin-binding domain, while nesprin3 is known to lack an actin-binding domain and binds instead primarily to intermediate filaments. However, recent work by Lu et al. shows that nesprin3 is able to functionally associate with the actin-binding domains of nesprins 1 and 2 and may support our findings[37]. Additionally, lamin A/C depletion had by far the strongest effect on actin cap formation of any of our knockdowns and had a notably higher impact than both nesprin2giant and nesprin3 depletion. We believe this could be due to the fact that LINC complexes have been shown to be "fluid" in nature[38]. Nesprin2giant is able overcompensate when nesprin3 is depleted, and *vice versa*[22]. After depletion of one of the nesprins, the other may have been able to overcompensate and help to put together some moderate organization of actin. Without lamin A/C, however, the cells were unable to respond at all.

In contrast to actin-cap fibers, which are physically anchored to the nuclear lamina through LINC complexes at the nuclear envelope, basal stress fibers have no direct connections to the nucleus. Therefore, we speculate that low shear stresses only activate the actin cap-based physical pathway described above, while high shear stresses engage both this LINC/actin-cap-based physical pathway and previously established biochemical pathways[2].

While a physical pathway mediating mechanotransduction has been long speculated to exist and is believed to involve focal adhesions and the actin network[18,39], these results identify that only a small subset of actin filaments – the LINC-anchored perinuclear actin-cap fibers – both directly connect to the nuclear lamina and participate in cellular response to flow-induced shear stresses.

## Methods

**Cell culture.** Wildtype and lamin knockout MEFs (a generous gift from Colin Stewart, Astar, Singapore) were cultured in DMEM (Mediatech) supplemented with 10% fetal bovine serum (FBS) (HyClone) and 100 units of penicillin/100 μg of streptomycin (Sigma). Cell media for cells knocked down of proteins of interest were supplemented with puromycin (Sigma): 3 μg/ml for MEFs depleted of focal adhesion proteins and 10 μg/ml for C2C12 siRNA scramble cells and nesprin2giant-depleted and nesprin3-depleted cells. Focal adhesion proteins were knocked down and confirmed as described previously[20] and nesprin proteins were knocked down and confirmed as described previously[22]. For both sets of knockdowns, multiple shRNA directed against each of our targeted proteins were used, and only the sequences showing more than 85% knocking down efficiency were chosen for experiments. All cells were maintained at 37°C in a humidified, 5% $CO_2$ environment. Cells were passaged every 2–3 days for a maximum of 20 passages.

75 x 38 x 1 mm glass slides (Fisher Scientific) were rinsed with ethanol and PBS (Gibco) before being coated with rat tail collagen type I (BD Biosciences) for 1 hour at a concentration of 50 μg/ml, a saturated concentration such that the amount of adsorbed collagen on the surface becomes independent of the bulk collagen concentration. Cells were seeded in DMEM with 5% serum and pen/strep. After 16 h, cells were rinsed once with Hank's Balanced Salt Solution (Gibco) and immersed in serum-free DMEM with pen/strep for 48 h before being fixed or sheared.

**Shear flow assay.** A parallel-plate flow chamber (GlycoTech) was placed on top of cell-seeded glass slides using a 0.127-mm thickness gasket with flow width of 2.5 mm. The wall shear stress produced by the flow, $\tau_w$ (dyn/cm$^2$), was calculated with the Navier-Stokes equation for Newtonian fluid flow between parallel plates, $\tau_w = 6\ \mu Q/a^2b$, where μ is the apparent viscosity of the flow medium at 37°C (in Poise), Q is the volumetric flow rate (in ml/sec), a is the gasket thickness (in cm), and b is the gasket width (in cm). The flow medium used was serum-free, in order to monitor physical responses independently from any biochemical responses, and consisted of DMEM, pen/strep, and 25 mM HEPES (Gibco) to act as a buffering agent. Flow medium was kept at 37°C using a heated water bath. Lines of the flow apparatus were primed with heated flow medium before shear experiments.

**Drug treatments.** Myosin light chain kinase (MLCK) inhibitor ML7 (Sigma) and myosin II inhibitor blebbistatin (Sigma) were dissolved in stock DMSO and were then added to the 5% serum and serum-free media for a final drug concentration of 25 μM. Rho-kinase (ROCK) inhibitor Y-27632 (Sigma) was dissolved in sterile water and added to the medium also for a final drug concentration of 25 μM. Cells were incubated with all drug media for 30 min before fixation (control experiments) or shear experiments. For shear experiments with drugs, serum-free flow medium contained the drug of interest at the same concentration as the drug culture medium (25 μM). Control experiments were performed with drug-free medium containing DMSO at the same concentration as in the drug medium to assure that DMSO was not affecting actin organization (not shown). It was assumed that the minute amount of sterile water used to dissolve Y-27642 did not affect actin organization.

**Immunofluorescence microscopy.** Immediately after control and shear experiments, cells were fixed in 3.7% formaldehyde for 10 min. Cells were subsequently permeabilized with 0.1% Triton X-100 for 10 min and blocked with 10% goat serum in PBS for 1 hour. Alexa-Fluor phalloidin 488 (Invitrogen) was used

to visualize actin filament organization at a 1 : 40 dilution, and ProLong® Gold antifade reagent with DAPI (Invitrogen) was used to visualize the nucleus. Fluorescent images were collected using either a Cascade 1 K CCD camera (Roper Scientific) or Luca-R EMCCD camera (Andor Technology) mounted on a Nikon TE2000 microscope with a 60x Plan Fluor lens (N.A. 1.4), or a Nikon A1 laser-scanning confocal microscope. Confocal images were processed using Nikon Elements software. Actin filament organization was manually assessed using the scoring assay explained in Fig. 1 with constant exposure time used for all conditions. Only single cells not in contact with any other cells were characterized[17].

**Statistical analysis.** Mean values, standard error of measurement, and statistical analysis for all data shown were calculated and plotted using Graphphad Prism (Graphpad Software). All bars and data points show mean and SEM values of two to three independent experiments. For actin cap and basal actin scoring, at least 50 cells in triplicate for a total of 150 cells were examined for all conditions. Where appropriate, the following statistical analyses were used to compare means: two-tailed unpaired *t*-tests, one-way ANOVA analyses with Tukey post-tests, and two-way ANOVA analyses with Bonferroni post-tests. In all data shown, ***, **,*, and ns indicate p value $<0.001$, $<0.01$, $<0.05$, and $>0.05$, respectively. The significance value $\alpha=0.05$ was used for all significance tests.


1. Davies, P. F. Flow-mediated endothelial mechanotransduction. *Physiol Rev* **75**, 519–560 (1995).
2. Tzima, E. *et al.* A mechanosensory complex that mediates the endothelial cell response to fluid shear stress. *Nature* **437**, 426–431 (2005).
3. Berlin, C. *et al.* alpha 4 integrins mediate lymphocyte attachment and rolling under physiologic flow. *Cell* **80**, 413–422 (1995).
4. Campbell, J. J. *et al.* Chemokines and the arrest of lymphocytes rolling under flow conditions. *Science* **279**, 381–384 (1998).
5. Hove, J. R. *et al.* Intracardiac fluid forces are an essential epigenetic factor for embryonic cardiogenesis. *Nature* **421**, 172–177 (2003).
6. Datta, N. *et al.* In vitro generated extracellular matrix and fluid shear stress synergistically enhance 3D osteoblastic differentiation. *Proceedings of the National Academy of Sciences of the United States of America* **103**, 2488–2493 (2006).
7. Healy, Z. R. *et al.* Divergent responses of chondrocytes and endothelial cells to shear stress: cross-talk among COX-2, the phase 2 response, and apoptosis. *Proceedings of the National Academy of Sciences of the United States of America* **102**, 14010–14015, doi:10.1073/pnas.0506620102 (2005).
8. Lee, J. S., Chang, M. I., Tseng, Y. & Wirtz, D. Cdc42 mediates nucleus movement and MTOC polarization in Swiss 3T3 fibroblasts under mechanical shear stress. *Molecular biology of the cell* **16**, 871–880 (2005).
9. Malek, A. M., Alper, S. L. & Izumo, S. Hemodynamic shear stress and its role in atherosclerosis. *JAMA : the journal of the American Medical Association* **282**, 2035–2042 (1999).
10. Cunningham, K. S. & Gotlieb, A. I. The role of shear stress in the pathogenesis of atherosclerosis. *Laboratory investigation; a journal of technical methods and pathology* **85**, 9–23, doi:10.1038/labinvest.3700215 (2005).
11. Shi, Z. D., Ji, X. Y., Qazi, H. & Tarbell, J. M. Interstitial flow promotes vascular fibroblast, myofibroblast, and smooth muscle cell motility in 3-D collagen I via upregulation of MMP-1. *American journal of physiology. Heart and circulatory physiology* **297**, H1225–1234, doi:10.1152/ajpheart.00369.2009 (2009).
12. Miteva, D. O. *et al.* Transmural flow modulates cell and fluid transport functions of lymphatic endothelium. *Circ Res* **106**, 920–931.
13. Shields, J. D. *et al.* Autologous chemotaxis as a mechanism of tumor cell homing to lymphatics via interstitial flow and autocrine CCR7 signaling. *Cancer Cell* **11**, 526–538 (2007).
14. Pelham, R. J., Jr. & Wang, Y. Cell locomotion and focal adhesions are regulated by substrate flexibility. *Proceedings of the National Academy of Sciences of the United States of America* **94**, 13661–13665 (1997).
15. Wang, H. B., Dembo, M., Hanks, S. K. & Wang, Y. Focal adhesion kinase is involved in mechanosensing during fibroblast migration. *Proceedings of the National Academy of Sciences of the United States of America* **98**, 11295–11300 (2001).
16. Wozniak, M. A., Modzelewska, K., Kwong, L. & Keely, P. J. Focal adhesion regulation of cell behavior. *Biochimica et biophysica acta* **1692**, 103–119 doi:10.1016/j.bbamcr.2004.04.007 (2004).
17. Khatau, S. B. *et al.* A perinuclear actin cap regulates nuclear shape. *Proceedings of the National Academy of Sciences of the United States of America* **106**, 19017–19022 (2009).
18. Wang, N., Tytell, J. D. & Ingber, D. E. Mechanotransduction at a distance: mechanically coupling the extracellular matrix with the nucleus. *Nat Rev Mol Cell Biol* **10**, 75–82 (2009).
19. Khatau, S. B. *et al.* The differential formation of the LINC-mediated perinuclear actin cap in pluripotent and somatic cells. *PloS one* **7**, 36689, doi:10.1371/journal.pone.0036689 (2012).
20. Kim, D. H. *et al.* Actin cap associated focal adhesions and their distinct role in cellular mechanosensing. *Scientific reports* **2**, 555, doi:10.1038/srep00555 (2012).
21. Hotulainen, P. & Lappalainen, P. Stress fibers are generated by two distinct actin assembly mechanisms in motile cells. *Journal of Cell Biology* **173**, 383–394 (2006).
22. Khatau, S. B. *et al.* The distinct roles of the nucleus and nucleus-cytoskeleton connections in three-dimensional cell migration. *Scientific reports* **2**, 488, doi:10.1038/srep00488 (2012).
23. Zhang, Q. *et al.* Nesprins: a novel family of spectrin-repeat-containing proteins that localize to the nuclear membrane in multiple tissues. *Journal of cell science* **114**, 4485–4498 (2001).
24. Luxton, G. W., Gomes, E. R., Folker, E. S., Vintinner, E. & Gundersen, G. G. Linear arrays of nuclear envelope proteins harness retrograde actin flow for nuclear movement. *Science* **329**, 956–959, doi:10.1126/science.1189072 (2010).
25. Razafsky, D. & Hodzic, D. Bringing KASH under the SUN: the many faces of nucleo-cytoskeletal connections. *J Cell Biol* **186**, 461–472 (2009).
26. Borrego-Pinto, J. *et al.* Samp1 is a component of TAN lines and is required for nuclear movement. *Journal of cell science* **125**, 1099–1105, doi:10.1242/jcs.087049 (2012).
27. Morgan, J. T. *et al.* Nesprin-3 regulates endothelial cell morphology, perinuclear cytoskeletal architecture, and flow-induced polarization. *Molecular biology of the cell* **22**, 4324–4334, doi:10.1091/mbc.E11-04-0287 (2011).
28. Lombardi, M. L. *et al.* The interaction between nesprins and sun proteins at the nuclear envelope is critical for force transmission between the nucleus and cytoskeleton. *The Journal of biological chemistry* **286**, 26743–26753, doi:10.1074/jbc.M111.233700 (2011).
29. Colombelli, J. *et al.* Mechanosensing in actin stress fibers revealed by a close correlation between force and protein localization. *Journal of cell science* **122**, 1665–1679 (2009).
30. Yoshigi, M., Hoffman, L. M., Jensen, C. C., Yost, H. J. & Beckerle, M. C. Mechanical force mobilizes zyxin from focal adhesions to actin filaments and regulates cytoskeletal reinforcement. *J Cell Biol* **171**, 209–215 (2005).
31. Beningo, K. A., Dembo, M., Kaverina, I., Small, J. V. & Wang, Y. L. Nascent focal adhesions are responsible for the generation of strong propulsive forces in migrating fibroblasts. *J Cell Biol* **153**, 881–888 (2001).
32. Vasioukhin, V., Bauer, C., Yin, M. & Fuchs, E. Directed actin polymerization is the driving force for epithelial cell-cell adhesion. *Cell* **100**, 209–219 (2000).
33. Zamir, E. *et al.* Dynamics and segregation of cell-matrix adhesions in cultured fibroblasts. *Nat Cell Biol* **2**, 191–196 (2000).
34. Riveline, D. *et al.* Focal contacts as mechanosensors: externally applied local mechanical force induces growth of focal contacts by an mDia1-dependent and ROCK-independent mechanism. *J Cell Biol* **153**, 1175–1186 (2001).
35. Stewart-Hutchinson, P. J., Hale, C. M., Wirtz, D. & Hodzic, D. Structural requirements for the assembly of LINC complexes and their function in cellular mechanical stiffness. *Exp Cell Res* **314**, 1892–1905 (2008).
36. Hale, C. M. *et al.* Dysfunctional connections between the nucleus and the actin and microtubule networks in laminopathic models. *Biophys J* **95**, 5462–5475 (2008).
37. Lu, W. *et al.* Nesprin interchain associations control nuclear size. *Cellular and molecular life sciences : CMLS* **69**, 3493–3509, doi:10.1007/s00018-012-1034-1 (2012).
38. Ostlund, C. *et al.* Dynamics and molecular interactions of linker of nucleoskeleton and cytoskeleton (LINC) complex proteins. *Journal of cell science* **122**, 4099–4108, doi:10.1242/jcs.057075 (2009).
39. Ingber, D. E. Mechanobiology and diseases of mechanotransduction. *Ann Med* **35**, 564–577 (2003).


## Acknowledgements

This work was supported by NIH grants R01GM084204 and U54CA143868, and a Research Grant from the Muscular Dystrophy Association (DH). ABC and SBK were supported by IGERT-NSF graduate fellowships. The authors thank Dr. Yungfeng Feng for providing focal adhesion protein knockdown cell lines. Publication of this article was funded in part by the Open Access Promotion Fund of the Johns Hopkins University Libraries.

## Author contributions

A.B.C., S.B.K., D.H., G.D.L. and D.W. designed the experiments. A.B.C., S.B.K., N.E. and D.K.R. conducted the experiments and analyzed the data. D.H. and G.D.L. provided new reagents. A.B.C. and D.W. wrote the paper. A.B.C., S.B.K., D.H., G.D.L. and D.W. edited the paper.

## Additional information

**Supplementary information** accompanies this paper at http://www.nature.com/scientificreports

**Competing financial interests:** The authors declare no competing financial interests.



**How to cite this article:** Chambliss, A.B. *et al.* The LINC-anchored actin cap connects the extracellular milieu to the nucleus for ultrafast mechanotransduction. *Sci. Rep.* **3**, 1087; DOI:10.1038/srep01087 (2013).